

Dynamics of self-interstitial structures in body-centred-cubic W studied by molecular dynamics simulation

This article has been downloaded from IOPscience. Please scroll down to see the full text article.

2000 J. Phys.: Condens. Matter 12 79

(<http://iopscience.iop.org/0953-8984/12/1/307>)

View [the table of contents for this issue](#), or go to the [journal homepage](#) for more

Download details:

IP Address: 171.66.16.218

The article was downloaded on 15/05/2010 at 19:25

Please note that [terms and conditions apply](#).

Dynamics of self-interstitial structures in body-centred-cubic W studied by molecular dynamics simulation

M H Carlberg[†], E P Münger and L Hultman

Linköping Institute of Technology, Department of Physics and Measurement Technology,
S-58183 Linköping, Sweden

E-mail: mcg@ifm.liu.se (M H Carlberg)

Received 27 August 1999

Abstract. This study concerns a molecular dynamics (MD) simulation, using the embedded-atom method (EAM), of the self-diffusion of an interstitial in the bcc metal tungsten (W) at 2000 K. It is found that the interstitial moves only along $\langle 111 \rangle$ diagonals and that the switches to other non-parallel directions take place through a two-dimensional process. The $\langle 011 \rangle$ dumb-bell is central to this process. Movement along the $\langle 111 \rangle$ diagonals takes place through $\langle 111 \rangle$ crowdions occupying 2–6 lattice sites. The probabilities of a direction switch and a move are 0.249 and 0.751, respectively. Translating the complicated movement mechanism into the simple picture of interstitial hopping between lattice points, the diffusion velocity is calculated to be 520 m s^{-1} , and the activation energy for the interstitial self-diffusion is calculated to be 0.54 eV/interstitial.

1. Introduction

Atomistic simulations of metallic materials have been performed since the late 1940s [1, 2] to investigate phenomena that could not readily be revealed by experiments. Molecular dynamics, MD, has been used to the same end for about as long, and since the advent of the Verlet algorithm in 1967 [3], it has been a standard method. But it was not until the early 1980s, when the embedded-atom method [4–6] (EAM), with its natural inclusion of many-body effects, was presented, that large systems could be simulated with confidence. Today, MD in conjunction with the EAM is used to study a wide variety of phenomena and materials, e.g. multilayers of Fe/Ag and Cu/Pd [7], annihilation of screw dislocations [8], martensitic transformations in Fe/Ni alloys [9], high-energy cascades [10], orders and structures of liquid and amorphous metals under solidification [11], liquid aluminium [12], metal–semiconductor interfaces [13], and point defects and clusters in hcp metals [14].

Diffusion is a phenomenon of great scientific and technological importance, as it impacts on almost every property of a material, and influences many important processes, like nuclear and chemical reactions, electrical resistivity, and transport of heat. The exact mechanism of diffusion on an atomistic level is hard to study experimentally, as the timescales involved are short and the spatial extents of the defect configurations are small. Naturally, the larger the defect complex the easier it is to study experimentally, as it becomes both easier to detect with methods such as positron annihilation spectroscopy and electron microscopy, and less mobile. To obtain detailed information, atomistic simulations can be applied successfully, provided

[†] Author to whom any correspondence should be addressed. Telephone: +46 13 281266; fax: +46 13 132285.

that the interaction potential used is suitable. This paper reports the result from such a study where the diffusion of a single interstitial in bcc W is studied using the EAM and MD.

2. Methodology

The simulation configuration was generated by taking a cube with a side of 12 unit cells, on which bulk conditions were imposed by using periodic boundary conditions in all three spatial directions. The mean pressure was reduced to zero by adjusting the size of the simulation cell. After the pressure had been adjusted, a single interstitial was added in the centre of the cell, in such a way that it was initially on the main $[111]$ diagonal in the middle between two other atoms on the same diagonal. This gave a total of 3457 atoms in the simulation cell. The temperature was set to 2000 K and the whole simulation cell was allowed to relax for 1 ps. After this, a further 500 ps were simulated which were then investigated.

The reported simulation was carried out by molecular dynamics, using the embedded-atom method [15] (EAM) to describe the interaction between the atoms. The forms used were those given by Johnson and Oh [5]. The total energy, the volume, and the number of particles were kept constant throughout the simulation, thus placing it in the thermodynamic EVN ensemble. The time step was dynamically adjusted so as to improve performance while conserving the total energy. Other details on the implementation can be found in previous work by the authors [16].

3. Results and discussion

3.1. Defect configurations

There are two types of defect observed in the simulation: a $\langle 011 \rangle$ dumb-bell and a $\langle 111 \rangle$ crowdion. The crowdion exists in several varieties, all having in common that X atoms share $X - 1$ lattice sites along an $\langle 111 \rangle$ direction. Those will be denoted as C_X , where X ranges from three to seven; C_3 is the crowdion familiar from the literature. For details on the defect configurations, see other work by the authors [20].

3.2. Movement of crowdions

Earlier simulations by the authors reveal that the interstitial is accommodated into the lattice through small distortions [20]. In this way, the interstitial stops being a perfect point defect, and gets a spatial extent. The movement of the interstitial is then not simply the jumping of a single atom through the lattice, but a subtle continuous movement through small rearrangements of a set of atoms.

The crowdions are located on a $\langle 111 \rangle$ direction. There are eight such in the bcc lattice, namely $[111]$, $[\bar{1}\bar{1}\bar{1}]$, $[\bar{1}11]$, $[1\bar{1}\bar{1}]$, $[1\bar{1}1]$, $[\bar{1}\bar{1}1]$, $[\bar{1}1\bar{1}]$, and $[11\bar{1}]$. Grouping these according to what $\langle 111 \rangle$ diagonal they are located on, and picking those with positive z -component, leaves four: $[111]$, $[\bar{1}\bar{1}1]$, $[1\bar{1}1]$, and $[\bar{1}1\bar{1}]$.

Consider the group of atoms that lie along a specific single $\langle 111 \rangle$ direction. The movement of the defect is restricted to this group of atoms. It will not involve atoms in any other parallel $\langle 111 \rangle$ directions. There is a single mechanism through which the crowdion can change over to another $\langle 111 \rangle$ direction. This is a two-dimensional process in the $\langle 011 \rangle$ plane defined by the two $\langle 111 \rangle$ directions involved. The process involves the dumb-bell and is described in detail further on in section 3.4.

When the crowdion moves along the $\langle 111 \rangle$ direction that it currently occupies, it does so through small rearrangements and distortions as described below, where the individual atoms move much less than half a unit-cell diagonal. A specific crowdion can either move by itself, or by first transforming to a larger crowdion, and then re-emerging somewhere along the extent of that. A C_x crowdion will, when it transforms, do so either to a C_{x-1} or to a C_{x+1} , apart from C_7 which only transforms into C_6 . The larger crowdions are as mobile as the smaller. The larger mass involved is compensated for by the smaller movement needed of the individual atoms in this case.

The movement of a C_4 crowdion one unit cell along a $\langle 111 \rangle$ direction is shown in figure 1. The C_4 crowdion transforms into a C_5 crowdion, which moves through the typical small rearrangements, and then the C_4 crowdion reappears at the upper end. This worm-like way of moving through extension and contraction is typical of the movement of the defect through the lattice.

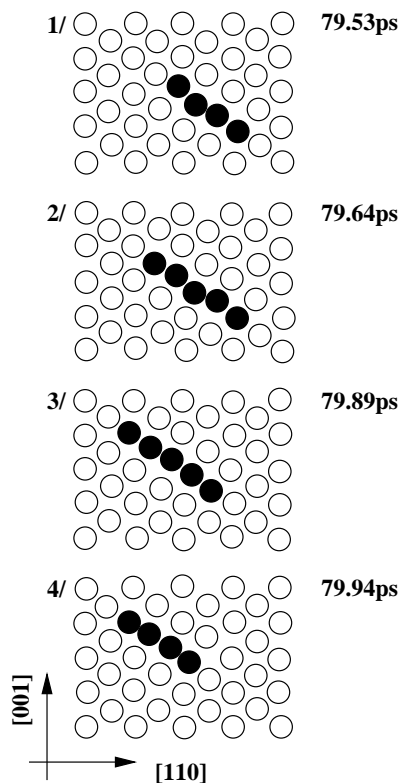


Figure 1. The figure shows how a C_4 crowdion moves a whole unit cell along a $\langle 111 \rangle$ direction through transforming into a C_5 crowdion, which moves through small rearrangements, and that the C_4 crowdion reappears at the upper end. The times are 79.53 ps, 79.64 ps, 79.89 ps, and 79.94 ps for panels (1), (2), (3), and (4) respectively. The atoms in the defect configuration are shown in black to aid the eye in discerning their motion.

3.3. Movement of the dumb-bell

The $\langle 011 \rangle$ dumb-bell does not move by itself, but rather transforms into a C_3 crowdion which then moves along an $\langle 111 \rangle$ direction using the movement mechanism of the crowdions as

shown in section 3.2. A process through which the dumb-bell in effect moves half a unit cell down along the $\langle 111 \rangle$ direction is shown in figure 2. First, the dumb-bell transforms into a C_3 , which then expands to the C_4 crowdion, which transforms into C_5 . The expansion continues through C_6 , into C_7 . The crowdion then contracts through C_6 to C_5 , and then through C_4 and C_3 back into the dumb-bell configuration—but half a unit-cell diagonal down along the $\langle 111 \rangle$ direction.

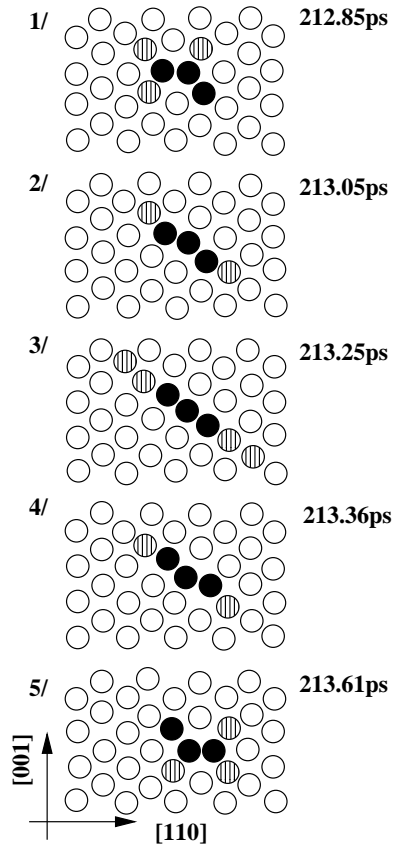


Figure 2. The figure shows how a dumb-bell moves half a unit cell along a $\langle 111 \rangle$ direction through C_3 to C_7 ; for brevity, only the steps involving the crowdions C_5 and C_7 are shown here. The times are 212.85 ps, 213.05 ps, 213.25 ps, 213.36 ps, and 213.61 ps for panels (1), (2), (3), (4), and (5) respectively. The atoms shown hatched are part of the defect. The atoms shown in black are part of the defect configuration in all panels; note their relative positions.

3.4. Rotation

There are two $\langle 111 \rangle$ diagonals passing through the middle of the $\langle 011 \rangle$ dumb-bell. Due to the symmetry of the configuration, the dumb-bell may transform into a crowdion on any one of them with the same probability with no preference for one or the other. For example, the centre of the dumb-bell in the $[1\bar{1}0]$ plane in figure 2 lies on the $[111]$ and $[\bar{1}\bar{1}1]$ diagonals. For the same reasons the crowdion can transform into a dumb-bell on any of the three $\{011\}$ planes of which the diagonal is part. For example, the crowdion of panel (3) in figure 2 could just as well have transformed into a dumb-bell on the (101) and (011) planes instead of on

the $(\bar{1}10)$ plane. Thus, the $\langle 011 \rangle$ dumb-bell is the central point through which the defect can change its direction of movement, and this can happen without the defect contracting to a real point defect.

The process is contained in the $\langle 011 \rangle$ plane defined by the starting and ending $\langle 111 \rangle$ diagonals. It is shown schematically in figure 3, leaving out some intermediate steps like the transformation of the dumb-bell into C_3 , and the transformation between the crowdions C_3 , C_4 , C_5 , and C_6 . The two central atoms (shown in black in the figure) are rotated, around the crossing points of the two diagonals, by the surrounding lattice. The configuration goes from crowdion to dumb-bell, and then to a crowdion on the other diagonal.

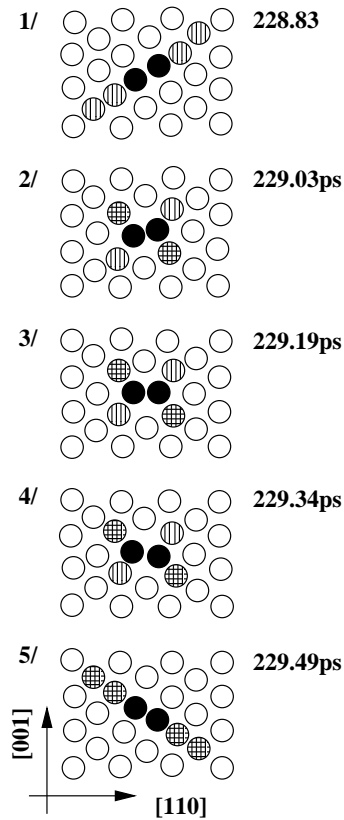


Figure 3. The figure shows the mechanism of crossover between two $\langle 111 \rangle$ directions in the same $\langle 011 \rangle$ plane, here the $[110]$ plane. A $[111]$ C_6 contracts into a dumb-bell configuration, which then expands into a C_6 along the $[11\bar{1}]$ diagonal. The times are 228.83 ps, 229.03 ps, 229.19 ps, 229.34 ps, and 229.49 ps in panels (1), (2), (3), (4), and (5) respectively. The atoms shown in black or hatched/cross-hatched are part of the defect. The atoms shown in black are part of the defect configuration in all panels and have been shown thus to emphasize their movement.

3.5. Simplified general movement

The above description of the movement of the defect configuration complex differs radically from the simple picture of the defect hopping between vacant neighbour sites found in much of the literature. The simplified picture can be arrived at by accounting for the interstitial at the centre of the distortion complex, and by accounting for the centre of the complex at

bcc lattice points. In this picture, for a single interstitial moving in a bcc lattice, there exist eight neighbouring sites to which the interstitial can jump. However, the restriction that the interstitial preferably moves along the current (111) direction must also be included. From the simulation, the probability of a move and a rotation are 0.751 and 0.249, respectively.

3.6. Diffusion constants

In the simplified picture where the interstitial moves through hopping to nearest-neighbour sites, the diffusion rate is [18]

$$\Gamma = z\nu e^{\Delta G/(RT)} \quad (1)$$

where Γ is the frequency of successful jumps, z is the number of sites to which the jump can be done, ν is the frequency of attempted jumps, $\Delta G = \Delta H - T \Delta S$ is the Gibbs free energy, R is the gas constant, and T is the temperature. The entropy term, $T \Delta S$, is zero, since there is just one interstitial in the simulation, and there are as many possible ways of placing it after the jump as before. The entity z is eight in a bcc lattice. Equation (1) can then be written as

$$\Gamma = 8\nu e^{\Delta H/(RT)}. \quad (2)$$

From this we can determine the enthalpy ΔH , which is the activation energy for the diffusion, if we can compute Γ and ν . The entity Γ is related to the average diffusion velocity, and ν is related to the movement of the atoms in the simulation.

By summing the length of the path along which the centre of the defect complex has moved, dividing the sum by the time elapsed, and plotting the resulting value as a function of the time, we arrive at figure 4. This gives, at the end of the simulation, an estimate of the diffusion velocity. From the figure, we estimate it to be 5.2 \AA ps^{-1} . The lattice constant in the simulation is 3.16 \AA , giving a nearest-neighbour distance of 2.74 \AA . The frequency of successful jumps is then $1.9 \times 10^{12} \text{ Hz}$.

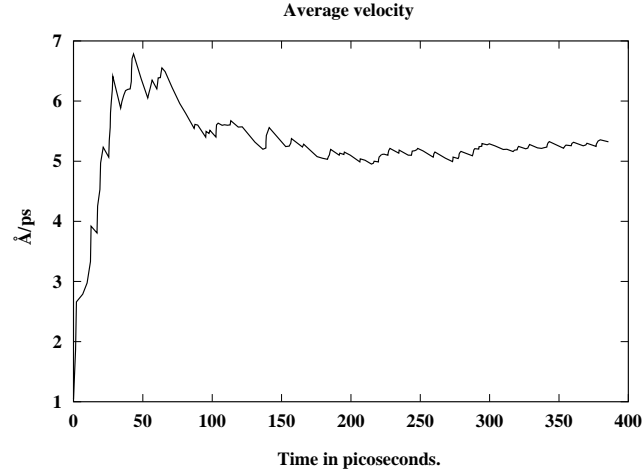


Figure 4. The figure shows the average diffusion velocity as a function of time. As more and more data are gathered into the average, the ‘noise’ decreases, and at the right-hand side of the figure, an estimation of the average diffusion velocity can be read.

The entity ν can be computed from the movement of the atoms through the simulation. Since the simulation has an adaptive time step, the data are not equidistant in time. This makes a direct Fourier transform impossible to perform; instead an estimation of the Fourier spectrum

was computed using the Lomb method [19]. The highest significant frequency in this spectrum was 5.3×10^{12} Hz.

It is now possible to compute ΔH from equation (2). The result is 51.7 kJ mol^{-1} , or 0.54 eV per interstitial atom. For self-diffusion through vacancies, the corresponding value from simulations is 5.54 eV/atom [17], and one experimental value is $5.63 \pm 0.21 \text{ eV}$ [17]. This is consistent with the immobility of vacancies as compared to self-interstitials observed generally in atomistic simulations and experiments. In a similar simulation to the one reported in this paper, but involving a vacancy, the defect does not move at all during the 500 ps simulated time.

The value of 0.54 eV per interstitial atom is clear in the simplified picture of an interstitial atom jumping between sites in the lattice. It is less so in the real configuration where the crowdion has been observed to contain up to seven atoms; is it then ‘ 0.54 eV per X atoms’? Since the movement process is so complex, it is hard to determine the energy barrier for every part of it. Thus the concept of an energy barrier is not very useful in this case.

4. Conclusions

Molecular dynamics using the EAM has been used to study the diffusion of a single interstitial in bcc W at 2000 K. The interstitial has a spatial extent and cannot be considered a point in space. Movement takes place only in the crowdion configuration, and only along the $\langle 111 \rangle$ direction that it currently occupies. The movement involves only delicate rearrangements of the atoms within the defect, and those directly outside of it on the same line. The crowdions transform only into the other crowdions of closest size apart from C_7 , which only transforms into C_6 , and C_3 , which might transform into C_4 or the dumb-bell. The dumb-bell is the central point through which another direction of movement occurs as it is the crossing point of non-parallel directions. The change to a new direction is a two-dimensional process in the plane defined by the two $\langle 111 \rangle$ directions involved. The probability of movement through crowdions, and change of direction through a dumb-bell, are 0.751 and 0.249, respectively.

The activation energy for the diffusion of a single interstitial in an otherwise defect-free matrix has been computed to be $0.54 \text{ eV/interstitial}$, which corresponds to a diffusion velocity of 520 m s^{-1} . This activation energy has been compared to the activation energy for diffusion through the vacancy mechanism and found to be a factor of ten lower. This is consistent with the general condition for crystals that vacancies are much less mobile than interstitials.

Acknowledgments

We acknowledge the support of the Material Research Consortium ‘Thin Film Growth’, financed by the Foundation for Strategic Research, SSF, and the Swedish Research Council for Engineering Science, TFR.

References

- [1] Metropolis N and Ulam S 1949 *J. Am. Stat. Assoc.* **44** 335
- [2] Metropolis N, Rosenbluth A W, Rosenbluth M N and Teller A H 1953 *J. Chem. Phys.* **21** 1097
- [3] Verlet L 1967 *Phys. Rev.* **127** 98
- [4] Finnis M W and Sinclair J E 1984 *Phil. Mag. A* **50** 45
Finnis M W and Sinclair J E 1986 *Phil. Mag. A* **53** 161 (erratum)
- [5] Johnson R A and Oh D J 1989 *J. Mater. Res.* **4** 1195
- [6] Foiles S M and Daw M S 1988 *Phys. Rev. B* **38** 12 643
- [7] Mazzone A M 1999 *Phil. Mag. B* **79** 625

- [8] Swaminarayan S, LeSaur R, Lomdahl P and Beazley D 1998 *J. Mater. Res.* **13** 3478
- [9] Entel P, Meyer R, Kadau K, Herper H C and Hoffman E 1998 *Euro. Phys. J. B* **5** 379
- [10] Alonso E, Caturla M J, Tang M, Huang H and Diaz de la Rubia T 1997 *Microstructure Evolution During Irradiation, Symp. Mater. Res. Soc.* (Pittsburgh, PA: Materials Research Society) p 367
- [11] Wang L, Liu H, Cheng K and Hu Z 1997 *Physica B* **239** 267
- [12] Cai J and Ye Y Y 1996 *Acta Phys. Sin.* **5** 431
- [13] Xuan L, Gefei Q and Wang E G 1999 *Phys. Rev. B* **59** 10 125
- [14] Bacon D J 1993 *J. Nucl. Mater.* **206** 249
- [15] Daw M and Baskes M I 1984 *Phys. Rev. B* **29** 6443
- [16] Carlberg M H, Münger E P and Chirita V 1996 *Phys. Rev. B* **54** 2217
- [17] Guellil A M and Adams J B 1992 *J. Mater. Res.* **7** 639
- [18] Porter D A and Easterling K E 1992 *Phase Transformations in Metals and Alloys* (London: Chapman and Hall)
- [19] Press W H, Teukolsky S A, Vetterling W T and Flannery B P 1989 *Numerical Recipes in FORTRAN* 2nd edn (New York: Cambridge University Press)
- [20] Carlberg M H, Münger E P and Hultman L 1999 *J. Phys.: Condens. Matter* **11** 6509